

The linear stability of a developing thermal front in a porous medium: The effect of local thermal non-equilibrium

Ali Nouri-Borujerdi^{a,*}, Amin R. Noghrehabadi^{a,b}, D. Andrew S. Rees^b

^a School of Mechanical Engineering, Sharif University of Technology, Tehran, Iran

^b Department of Mechanical Engineering, University of Bath, Bath BA2 7AY, UK

Received 5 October 2006

Available online 27 March 2007

Abstract

In this paper we analyze the stability of the developing thermal boundary layer which is induced by a step-change in the temperature of the lower horizontal boundary of a uniformly cold semi-infinite porous medium. Particular attention is paid to the influence of local thermal non-equilibrium between the fluid and solid phases and how this alters the stability criterion compared with corresponding criterion when the phases are in local thermal equilibrium. A full linear stability analysis is developed without approximation, and this yields a parabolic system of equations for the evolving disturbances. Criteria for the onset of convection are derived as a function of the three available nondimensional parameters, the inter-phase heat transfer coefficient, H , the porosity-scaled conductivity ratio, γ , and the diffusivity ratio, α .

© 2007 Elsevier Ltd. All rights reserved.

Keywords: Convective instabilities; Linear theory; Porous media; Boundary layer; Thermal front; Local thermal non-equilibrium

1. Introduction

Much recent work has focused on the instability of convective flows in porous media. The reason is straightforward: if a computed flow turns out to be unstable, then it cannot be observed in practice, and important quantities, such as global rates of heat transfer, which are derived from such solutions can give misleadingly incorrect results. Therefore it is essential to examine all flows for their stability, and hence their realizability. It is with this in mind that we consider the stability of an evolving thermal front which is induced by suddenly raising the temperature of the lower horizontal boundary of what is essentially a semi-infinite porous region to a new constant level. It is well-known that the resulting conduction profile is described by the complementary error function when the medium is either purely

solid (in which case we refer back to the analysis of [1]) or when the medium is a fluid-saturated porous medium under conditions of local thermal equilibrium (LTE). In this latter case only one energy equation is required to model the temperature field, and in the absence of flow, the physical situation is exactly equivalent to the solid conduction problem described in [1].

The above scenario is potentially unstable, however, since hot fluid lies under cold fluid. As time progresses the thickness of this evolving thermal boundary layer increases with time, and if a Darcy–Rayleigh number, Ra , were to be defined using the instantaneous boundary layer thickness as a lengthscale, then Ra would also increase in time. Therefore the evolving conduction profile becomes increasingly susceptible to instability with the passage of time. The aim then is to determine the earliest time for which instability may arise. Such a situation has enormous practical importance for this type of convective instability could easily occur during the long-term underground storage of gas emissions from power stations described by

* Corresponding author.

E-mail address: anouri@sharif.edu (A. Nouri-Borujerdi).

Nomenclature

a	wavenumber of disturbance	γ	porosity-modified conductivity ratio
C	specific heat	ϵ	porosity
c.c.	complex conjugate	η	similarity variable
D	microscopic lengthscale	θ	fluid temperature
E	energy of disturbance	Θ	fluid temperature disturbance
g	gravity	μ	dynamic viscosity
h	inter-phase heat transfer coefficient	ρ	density
H	nondimensional form of h	σ	heat capacity ratio
k	conductivity	τ	scaled time
K	permeability	ϕ	solid temperature
L	natural lengthscale	Φ	solid temperature disturbance
P	pressure	ψ	streamfunction
Ra	Darcy–Rayleigh number	Ψ	streamfunction disturbance
t	time		
T	temperature		
u	horizontal velocity		
v	vertical velocity		
x	horizontal coordinate		
y	vertical coordinate		
<i>Greek symbols</i>			
α	thermal diffusivity ratio		
β	expansion coefficient		
<i>Superscripts and subscripts</i>			
0	initiation of disturbance		
∞	ambient/initial conditions		
basic	basic state		
c	neutral/critical conditions		
f, s	designating fluid or solid phase		
pm	porous medium		
w	wall/surface conditions		
–	dimensional		

Socolow [2]. Although CO₂ is a solute, the governing equations for mass transfer in an isothermal system are identical to those governing thermally induced convection in the absence of solute.

The study of this type of evolving stability problem is not new, and there have been a number of papers published on the topic. Morton [3] considered the rapid heating of a layer of clear fluid of finite thickness. The evolving conduction solution becomes unstable long before its thickness is comparable with the depth of the layer. Foster [4] revisited Morton's analysis using amplification theory, which is a time-dependent analysis. The onset of convection requires the use of an amplification factor to mark the onset of convection. Another method, called propagation theory, has been used by Hwang and Choi [5], Choi et al. [6] and Kim et al. [7] for convection in clear fluids, and by Kim et al. [8] for the instability of the flow induced by an impulsively started rotating cylinder. This latter theory employs the thermal penetration depth as a length scaling factor and then the linearized stability equations are transformed into self-similar form. The onset time is then determined as the eigenvalue of an ordinary differential eigenvalue problem. Bassom and Blennerhassett [9] also studied impulsively generated convection in a semi-infinite fluid layer above a heated flat plate using quasi-steady approximations to the disturbance equations to reduce the full partial differential disturbance equations to ordinary differential form. Experimental results have also been described by Goldstein and Volino [10].

Kaviani [11] extended amplification theory to convective flows in porous layers by suddenly imposing a uniform rate of heat generation within the layer. Kim et al. [12] also considered this internal heat generation problem where the basic state was still time-dependent and employed amplification theory. Later Kim et al. [13] considered an application to an oil-saturated medium with gas diffusion from below, while Kim and Kim [14] determined criteria for the onset of convection in a porous layer where the temperature of the lower surface increases linearly with time. Again, amplification theory is applied. Finally, it is essential to mention the work of Riaz et al. [15] who undertook both a linear stability analysis and strongly nonlinear simulations of the problem considered by Kim et al. [13]. In that paper the authors introduce an approximation, named the quasi-steady-state approximation, which allows the authors to determine the growth rates of individual modes at chosen times. This approximation is slightly different from that made in [13] and therefore the critical time and wavenumber they compute are also slightly different.

Recently Selim and Rees [16] revisited the problem of Kim et al. [13] and Riaz et al. [15] by examining the full linear stability problem without approximation. Therefore the stability characteristics were found by solving a parabolic system of partial differential equations. Disturbances were seeded at a chosen initiation time, and their evolution with time was monitored. From this process the onset of convection, which was defined as being the time when the rate of change of a thermal energy integral is zero, was found as a

function of the disturbance wavenumber, and a neutral stability curve was constructed from this information. The minimum critical time for instability was shown to be substantially earlier than those given by Kim et al. [13] and Riaz et al. [15]. This qualitative result is, perhaps, not surprising, as the imposition of an approximation (such as the reduction of a parabolic system to an ordinary differential system by neglecting time derivatives) is likely to make it more difficult for instability to arise. More specifically, the setting of a zero growth rate for the whole of the temperature profile does not account for the fact that the disturbance changes shape with time.

In the present paper we extend the work of Selim and Rees [16] by relaxing the assumption that the fluid and the porous matrix are in local thermal equilibrium. Consequently we use energy equations for the temperatures of each phase. These equations are coupled by source/sink terms which allow the transfer of heat from the hotter phase to the cooler phase. When LTE occurs, the basic conducting state is self-similar with an expanding thermal field, but when local thermal non-equilibrium (LTNE) occurs then even the basic state is nonsimilar and needs to be computed. Apart from this latter aspect, the general methodology followed here follows closely that of Selim and Rees [16].

2. Governing equations and basic solution

We are considering the thermo-convective instability of a semi-infinite region of saturated porous medium which is initially at the uniform temperature, T_∞ , but whose lower boundary has its temperature raised suddenly to a new uniform level, T_w . Darcy's law is assumed to apply within the porous medium, which is homogeneous and isotropic, and the fluid satisfies the Boussinesq approximation. However, we do not assume that there is local thermal equilibrium between the phases, and therefore we adopt the two-temperature model for which the evolution of the temperatures of the solid and fluid phases are modelled using separate energy equations. As in Selim and Rees [16], it is not necessary to consider the fully three-dimensional equations since the linearized disturbance equations may always be Fourier-decomposed into two-dimensional components of the form we consider later. Therefore the full two-dimensional equations of motion may be written in the form,

$$\frac{\partial \bar{u}}{\partial \bar{x}} + \frac{\partial \bar{v}}{\partial \bar{y}} = 0, \quad (1a)$$

$$\bar{u} = -\frac{K}{\mu} \frac{\partial \bar{P}}{\partial \bar{x}}, \quad (1b)$$

$$\bar{v} = -\frac{K}{\mu} \frac{\partial \bar{P}}{\partial \bar{y}} + \frac{\rho g \beta K}{\mu} (T_f - T_\infty), \quad (1c)$$

$$\begin{aligned} \epsilon(\rho c)_f \frac{\partial T_f}{\partial \bar{t}} + (\rho c)_f \left(\bar{u} \frac{\partial T_f}{\partial \bar{x}} + \bar{v} \frac{\partial T_f}{\partial \bar{y}} \right) \\ = \epsilon \nabla \cdot (k_f \nabla T_f) + h(T_s - T_f), \end{aligned} \quad (1d)$$

$$(1 - \epsilon)(\rho c)_s \frac{\partial T_s}{\partial \bar{t}} = (1 - \epsilon) \nabla \cdot (k_s \nabla T_s) + h(T_f - T_s) \quad (1e)$$

see Nield and Bejan [17] and Rees and Pop [18]. In these equations \bar{x} is the coordinate in the horizontal direction while \bar{y} is vertically upward. The corresponding velocities are \bar{u} and \bar{v} , respectively. All the other terms have their usual meaning for porous medium convection, and these are given in the Nomenclature. However, we single out the value h which is the dimensional inter-phase heat transfer coefficient. Little is known about how h varies with the conductivities and diffusivities of the phases, with the porosity and with the detailed geometry of the porous matrix. However, recent work by Rees [19] has shown that

$$h = \frac{28.4542}{D^2 \left(\frac{\epsilon}{k_f} + \frac{1-\epsilon}{k_s} \right)} \quad (2)$$

for a two-dimensional periodic chequerboard pattern in the absence of flow, where the pattern repeats over the microscopic lengthscale, D , and where the diffusivities of the phases are identical. Other porous structures were found to obey a similar formula where the 'constant of proportionality' is weakly dependent on ϵ , k_f and k_s .

There is no macroscopic lengthscale in this problem that may be used in the process of nondimensionalisation. However, we may define a natural lengthscale, L , by setting the Darcy-Rayleigh number, which is defined as $Ra = \rho g \beta K L (T_w - T_\infty) / \mu \alpha_{pm}$, to be equal to 1. This process is discussed in some detail in the review by Rees [20], and it is equivalent to defining a natural lengthscale based upon the fluid and matrix properties; thus a nondimensional length of precisely 1 is equivalent to the dimensional length, L , given by

$$L = \frac{\mu \alpha_{pm}}{\rho g \beta K (T_w - T_\infty)}. \quad (3)$$

Eqs. (1a)–(1e) may now be nondimensionalised using the following transformations:

$$\begin{aligned} \bar{t} &= \frac{L^2 \sigma}{\alpha_{pm}} t, \quad (\bar{x}, \bar{y}) = L(x, y), \quad (\bar{u}, \bar{v}) = \frac{\alpha_{pm}}{L} (u, v), \\ \bar{P} &= \frac{\alpha_{pm} \mu}{K} p, \end{aligned} \quad (4a)$$

and

$$T_f = T_\infty + (T_w - T_\infty)\theta, \quad T_s = T_\infty + (T_w - T_\infty)\phi, \quad (4b)$$

where

$$\sigma = \frac{(\rho C)_{pm}}{(\rho C)_f}, \quad \alpha_{pm} = \frac{k_{pm}}{(\rho C)_f} \quad (5a)$$

and

$$(\rho C)_{pm} = (1 - \epsilon)(\rho C)_s + \epsilon(\rho C)_f, \quad k_{pm} = (1 - \epsilon)k_s + \epsilon k_f. \quad (5b)$$

These substitutions yield the following system of equations:

$$\frac{\partial u}{\partial x} + \frac{\partial v}{\partial y} = 0, \tag{6a}$$

$$u = -\frac{\partial p}{\partial x}, \tag{6b}$$

$$v = -\frac{\partial p}{\partial y} + \theta, \tag{6c}$$

$$\begin{aligned} &\left(\frac{\gamma+1}{\gamma+\alpha}\right) \frac{\partial \theta}{\partial t} + \left(\frac{\gamma+1}{\gamma}\right) \left(u \frac{\partial \theta}{\partial x} + v \frac{\partial \theta}{\partial y}\right) \\ &= \frac{\partial^2 \theta}{\partial x^2} + \frac{\partial^2 \theta}{\partial y^2} + H(\phi - \theta), \end{aligned} \tag{6d}$$

$$\alpha \left(\frac{\gamma+1}{\gamma+\alpha}\right) \frac{\partial \phi}{\partial t} = \frac{\partial^2 \phi}{\partial x^2} + \frac{\partial^2 \phi}{\partial y^2} + H\gamma(\theta - \phi). \tag{6e}$$

The appropriate boundary conditions are

$$y = 0: \quad v = 0, \quad \theta = 1 \quad \text{and} \quad y \rightarrow \infty: \quad v, \theta \rightarrow 0, \tag{7}$$

while $\theta = 0$ everywhere for $t < 0$.

After eliminating the pressure, p , between Eqs. (6b) and (6c), the streamfunction, ψ , may be defined according to

$$u = -\frac{\partial \psi}{\partial y} \quad \text{and} \quad v = \frac{\partial \psi}{\partial x}, \tag{8}$$

in order to satisfy the continuity equation, and so Eqs. (6b)–(6e) reduce to the system,

$$\frac{\partial^2 \psi}{\partial x^2} + \frac{\partial^2 \psi}{\partial y^2} = \frac{\partial \theta}{\partial x}, \tag{9a}$$

$$\begin{aligned} &\left(\frac{\gamma+1}{\gamma+\alpha}\right) \frac{\partial \theta}{\partial t} + \left(\frac{\gamma+1}{\gamma}\right) \left(\frac{\partial \psi}{\partial x} \frac{\partial \theta}{\partial y} - \frac{\partial \psi}{\partial y} \frac{\partial \theta}{\partial x}\right) \\ &= \frac{\partial^2 \theta}{\partial x^2} + \frac{\partial^2 \theta}{\partial y^2} + H(\phi - \theta), \end{aligned} \tag{9b}$$

$$\alpha \left(\frac{\gamma+1}{\gamma+\alpha}\right) \frac{\partial \phi}{\partial t} = \frac{\partial^2 \phi}{\partial x^2} + \frac{\partial^2 \phi}{\partial y^2} + H\gamma(\theta - \phi), \tag{9c}$$

which are to be solved subject to the boundary conditions,

$$y = 0: \quad \psi = 0, \quad \theta = 1 \quad \text{and} \quad y \rightarrow \infty: \quad \psi, \theta \rightarrow 0. \tag{9d}$$

In Eqs. (9a)–(9c) the nondimensional parameters, α , H and γ are defined according to

$$\alpha = \frac{k_f}{(\rho C)_f} \frac{(\rho C)_s}{k_s}, \quad H = \frac{hL^2}{\epsilon k_f}, \quad \gamma = \frac{\epsilon k_f}{(1 - \epsilon)k_s}, \tag{10}$$

which are a diffusivity ratio, an inter-phase heat transfer coefficient and a porosity-weighted conductivity ratio.

Finally, we transform the y and t coordinates according to

$$\eta = \frac{y}{2\sqrt{t}}, \quad \tau = \sqrt{t}, \tag{11}$$

and therefore Eqs. (9) become

$$4\tau^2 \frac{\partial^2 \psi}{\partial x^2} + \frac{\partial^2 \psi}{\partial \eta^2} = 4\tau^2 \frac{\partial \theta}{\partial x}, \tag{12a}$$

$$\begin{aligned} &2\tau \left(\frac{\gamma+1}{\gamma+\alpha}\right) \frac{\partial \theta}{\partial \tau} + 2\tau \left(\frac{\gamma+1}{\gamma}\right) \left(\frac{\partial \psi}{\partial x} \frac{\partial \theta}{\partial \eta} - \frac{\partial \psi}{\partial \eta} \frac{\partial \theta}{\partial x}\right) \\ &= 4\tau^2 \frac{\partial^2 \theta}{\partial x^2} + \frac{\partial^2 \theta}{\partial \eta^2} + 2\eta \left(\frac{\gamma+1}{\gamma+\alpha}\right) \frac{\partial \theta}{\partial \eta} + 4\tau^2 H(\phi - \theta), \end{aligned} \tag{12b}$$

$$\begin{aligned} &2\tau \alpha \left(\frac{\gamma+1}{\gamma+\alpha}\right) \frac{\partial \phi}{\partial \tau} = 4\tau^2 \frac{\partial^2 \phi}{\partial x^2} + \frac{\partial^2 \phi}{\partial \eta^2} + 2\eta \alpha \left(\frac{\gamma+1}{\gamma+\alpha}\right) \frac{\partial \phi}{\partial \eta} \\ &\quad + 4\tau^2 H\gamma(\theta - \phi). \end{aligned} \tag{12c}$$

The basic state, whose stability characteristics form the purpose of the present paper, may be found by solving those equations which arise when the x -derivatives in (12) are suppressed

$$\frac{\partial^2 \psi}{\partial \eta^2} = 0, \tag{13a}$$

$$2\tau \left(\frac{\gamma+1}{\gamma+\alpha}\right) \frac{\partial \theta}{\partial \tau} = \frac{\partial^2 \theta}{\partial \eta^2} + 2\eta \left(\frac{\gamma+1}{\gamma+\alpha}\right) \frac{\partial \theta}{\partial \eta} + 4\tau^2 H(\phi - \theta), \tag{13b}$$

$$2\tau \alpha \left(\frac{\gamma+1}{\gamma+\alpha}\right) \frac{\partial \phi}{\partial \tau} = \frac{\partial^2 \phi}{\partial \eta^2} + 2\eta \alpha \left(\frac{\gamma+1}{\gamma+\alpha}\right) \frac{\partial \phi}{\partial \eta} + 4\tau^2 H\gamma(\theta - \phi). \tag{13c}$$

Given the form of (13a) it is clear that there is no flow associated with the basic state. The remaining equations for θ and ϕ do not admit self-similar solutions in general, unlike when the phases are in LTE (or when $\alpha = 1$, i.e. the diffusivities of the phases are equal), and therefore it is necessary to compute the basic state. Such computations have already been presented in the paper by Nouri-Borujerdi et al. [21] and shall not be repeated here. However we may quote the following results:

$$\theta \sim \operatorname{erfc} \left[\left(\frac{\gamma+1}{\gamma+\alpha}\right)^{0.5} \eta \right] \quad \text{and} \quad \phi \sim \operatorname{erfc} \left[\left(\alpha \frac{\gamma+1}{\lambda+\alpha}\right)^{0.5} \eta \right], \tag{14a, b}$$

when $\tau \ll 1$, and that

$$\theta \sim \operatorname{erfc}(\eta), \quad \phi \sim \operatorname{erfc}(\eta), \tag{15}$$

when $\tau \gg 1$. Therefore we may state that LTNE effects are strong at early times when the coefficients of $(\theta - \phi)$ in (13) are small. From (14) it is clear that the thermal boundary layer corresponding to the fluid phase is thicker than that corresponding to the solid phase when $\alpha > 1$, and vice versa when $\alpha < 1$. But at late times the thermal profiles of the two phases are identical to leading order. In the remainder of the paper we will label the evolving basic states as θ_{basic} and ϕ_{basic} and these are computed using the Keller box method in the manner specified below.

3. Linear stability theory

We may now assess the stability characteristics of the evolving basic state using a straightforward perturbation theory. Therefore we set

$$\psi = i\Psi(\tau, \eta)e^{iax} + \text{c.c.}, \tag{16a}$$

$$\theta = \theta_{\text{basic}} + (\Theta(\tau, \eta)e^{iax} + \text{c.c.}), \tag{16b}$$

$$\phi = \phi_{\text{basic}} + (\Phi(\tau, \eta)e^{iax} + \text{c.c.}), \tag{16c}$$

where Ψ , Θ and Φ are of sufficiently small amplitude that nonlinear terms may be neglected. The value, a , is the horizontal wavenumber of the disturbances. Therefore we obtain the following system of linearized disturbance equations:

$$\Psi'' - 4\tau^2 a^2 \Psi = 4\tau^2 a \Theta, \tag{17a}$$

$$2\tau \left(\frac{\gamma+1}{\gamma+a}\right) \Theta_\tau = \Theta'' + 2\eta \left(\frac{\gamma+1}{\gamma+a}\right) \Theta' - 4\tau^2 a^2 \Theta + 2\tau \left(\frac{\gamma+1}{\gamma}\right) a \theta'_{\text{basic}} \Psi + 4\tau^2 H(\Phi - \Theta), \tag{17b}$$

$$2\alpha\tau \left(\frac{\gamma+1}{\gamma+a}\right) \Phi_\tau = \Phi'' + 2\alpha\eta \left(\frac{\gamma+1}{\gamma+a}\right) \Phi' - 4\tau^2 a^2 \Phi + 4\tau^2 H\gamma(\Theta - \Phi). \tag{17c}$$

Nouri-Borujerdi et al. [21] noted that H may be scaled out of the equations for the basic state (see Eqs. (13b) and (13c)). However, it is not possible to do that for the above disturbance equations, and therefore Eqs. (17) form a three-parameter system with α , H and γ as the governing nondimensional parameters. We follow the procedure used in Selim and Rees [16] by introducing a disturbance at an early time and by following the evolution of that disturbance. In that paper it was found that the thermal energy

of the disturbance, a global measure of its amplitude, yields an earlier critical time than does the surface rate of heat transfer, which is a local measure. Therefore we shall monitor the evolving disturbance by means of the quantity, E , which is defined as

$$E = \frac{1}{2} \int_0^\infty \left(\Theta + \frac{\alpha}{\gamma} \Phi\right) dy = \tau \int_0^\infty \left(\Theta + \frac{\alpha}{\gamma} \Phi\right) d\eta \tag{18}$$

and which may be termed a thermal energy.

4. Numerical simulations

Parabolic simulations of the system given by Eqs. (17) were undertaken using the Keller-box method, first introduced by Keller and Cebeci [22]. However, we use a backward difference discretization in τ , rather than a central difference approximation, in order to maximize numerical stability. In the present computations, uniform grids in both the τ and η -directions were used with a τ -step of 0.01, and an η -step of 0.05. The maximum value of η depended on the precise values of H , γ and α as the thickness of the thermal boundary layer depends on these parameters; see Eq. (14). The initial disturbance profiles were chosen to be

$$\Theta = \eta e^{-3\eta}, \quad \Phi = 0, \tag{19}$$

at a specified initiation time, τ_0 , and with a specified wavenumber, a . We note that the corresponding initial Ψ -profile is given uniquely by the solution of Eq. (17a), and, given

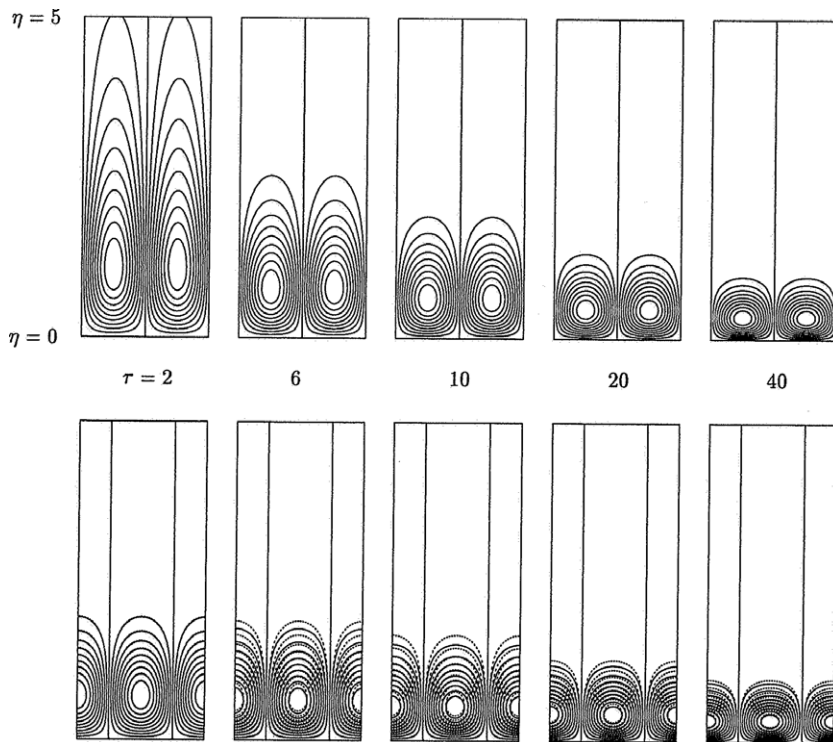


Fig. 1. Instantaneous streamlines (upper frames) and isotherms (lower frames) for $\tau_0 = 1$, $a_c = 0.15567$, $\alpha = 1$, $\gamma = 1$ and $H = 10^{-5}$ plotted in (x, η) -space. For the isotherms, continuous lines correspond to the fluid phase while dashed lines correspond to the solid phase. The critical time is given by $\tau_c = 4.44280$.

that the method uses backward differences, it is not necessary to find this initial profile.

Certain aspects of the the conclusions of Selim and Rees [16] also apply here, and therefore we shall not dwell upon demonstrating them again. However it is necessary to state that neither the initial temperature profiles nor their initiation time affect the time at which the disturbances become neutrally stable, although it must be stressed that this is true only when the initiation is sufficiently early. Here we have chosen $\tau_0 = 1$ which is sufficiently well before our calculated onset times.

Likewise, the evolution with time of the energy integral, E , exhibits precisely the same qualitative behaviour for any choice of the parameters, H , γ and α , as the analogous LTE computations of Selim and Rees [16]. But it is important to note that, for each parameter set, (H, γ, α) , there is a wave-number above which E is a monotonically decaying function of τ . This implies that the evolving thermal boundary layer is stable to all disturbances with such wavenumbers. On the other hand, at smaller wavenumbers, E decays at first, then experiences an interval of growth (the interval being longer for smaller values of a) and then it finally decays. This means that the disturbance has a finite interval of time during which growth may take place. Such a scenario happens for most boundary layers. On a practical level we determine the times at which $\partial E / \partial t = 0$ for each chosen wavenumber, and thereby these data form points on the neutral stability curve.

Table 1

Maximum values of the disturbance streamfunction and temperatures for the case, $\tau_0 = 1$, $a_c = 0.15567$, $\alpha = 1$, $\gamma = 1$, $H = 10^{-5}$, which is shown in Fig. 1

τ	$ \Psi \sin ax _{\max}$	$ \Theta \cos ax _{\max}$	$ \Phi \cos ax _{\max}$
2	0.1915	18.22×10^{-2}	5.000×10^{-6}
6	0.1512	4.772×10^{-2}	7.213×10^{-6}
10	0.3328	8.116×10^{-2}	15.31×10^{-6}
20	6.1005	195.5×10^{-2}	317.3×10^{-6}
40	3.5482	61.68×10^{-2}	270.3×10^{-6}

4.1. Evolution of the disturbances

Fig. 1 shows how the instantaneous streamlines and the isotherms evolve in time for the case $\gamma = 1$, $\alpha = 1$ and $H = 10^{-5}$. All frames are scaled so that there are 20 equal intervals between the maximum and minimum values of each of the three respective disturbance variables. Of chief interest here are (i) the changing thickness with time of the disturbances and (ii) the relative thickness of the fluid phase and solid phase disturbances.

With regard to (i), the disturbance becomes thinner (in terms of η) as time progresses. This behaviour may be traced to the presence of terms like $-4\tau^2 a^2 \Psi$ in Eq. (17a) which ensure that the e-folding distance of the exponential decay decreases with time. However, Fig. 2 of Selim and Rees [16], which also demonstrates this behaviour when the phases are in LTE, also shows that the thickness of

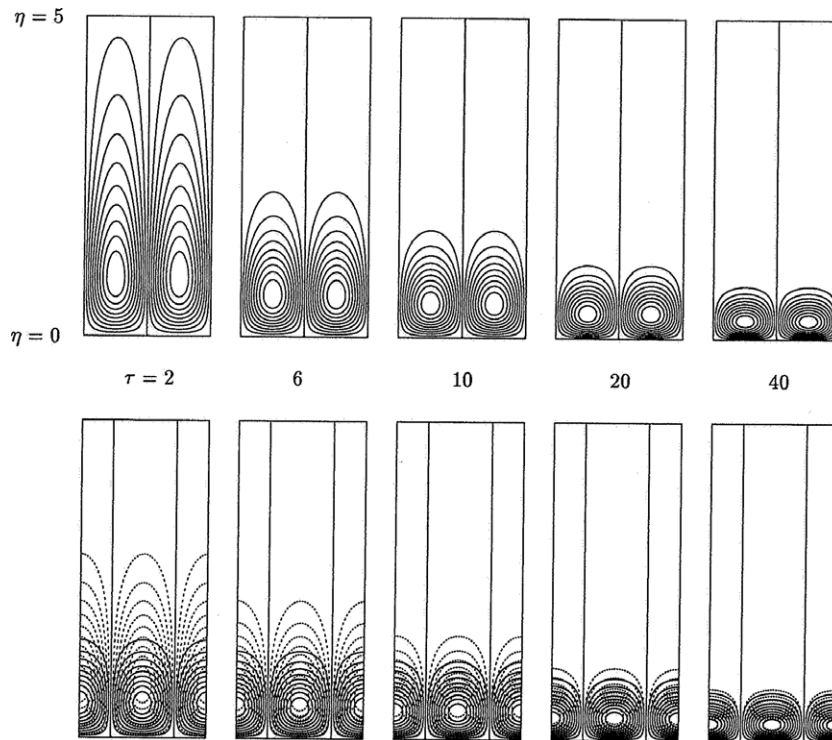


Fig. 2. Instantaneous streamlines (upper frames) and isotherms (lower frames) for $\tau_0 = 1$, $a_c = 0.16581$, $\alpha = 10^{-1}$, $\gamma = 1$, $H = 10^{-5}$ plotted in (x, η) -space. For the isotherms, continuous lines correspond to the fluid phase while dashed lines correspond to the solid phase. The critical time is given by $\tau_c = 5.98686$.

the disturbance in terms of y still increases very slightly with time.

Table 2
Maximum values of the disturbance streamfunction and temperatures for the case $\tau_0 = 1$, $a_c = 0.16581$, $\alpha = 10^{-1}$, $\gamma = 1$, $H = 10^{-5}$, which is shown in Fig. 2

τ	$ \Psi \sin ax _{\max}$	$ \Theta \cos ax _{\max}$	$ \Phi \cos ax _{\max}$
2	0.2098	27.53×10^{-2}	11.51×10^{-6}
6	0.1366	5.290×10^{-2}	8.769×10^{-6}
10	0.1817	5.056×10^{-2}	11.35×10^{-6}
20	1.4420	30.40×10^{-2}	90.09×10^{-6}
40	30.417	545.0×10^{-2}	196.4×10^{-6}

With regard to (ii), there is only a slight difference between the thicknesses of the thermal boundary layers of the respective phases. We believe that this is because $\alpha = 1$, and therefore the phases have identical thermal diffusivities. However, the amplitudes of the thermal disturbances are very substantially different from each other, as may be seen in Table 1, below. At $\tau = 2$ the amplitude of the thermal disturbance in the fluid phase is approximately 36,400 times larger than its solid phase counterpart. As time progresses this ratio decreases until, at $\tau = 40$, it is approximately 2280. This trend continues as τ increases because the source/sink terms, which are proportional to $\tau^2 H$ in Eqs. (17b) and (17c), become increasingly dominant. At very large times the two thermal fields become coincident

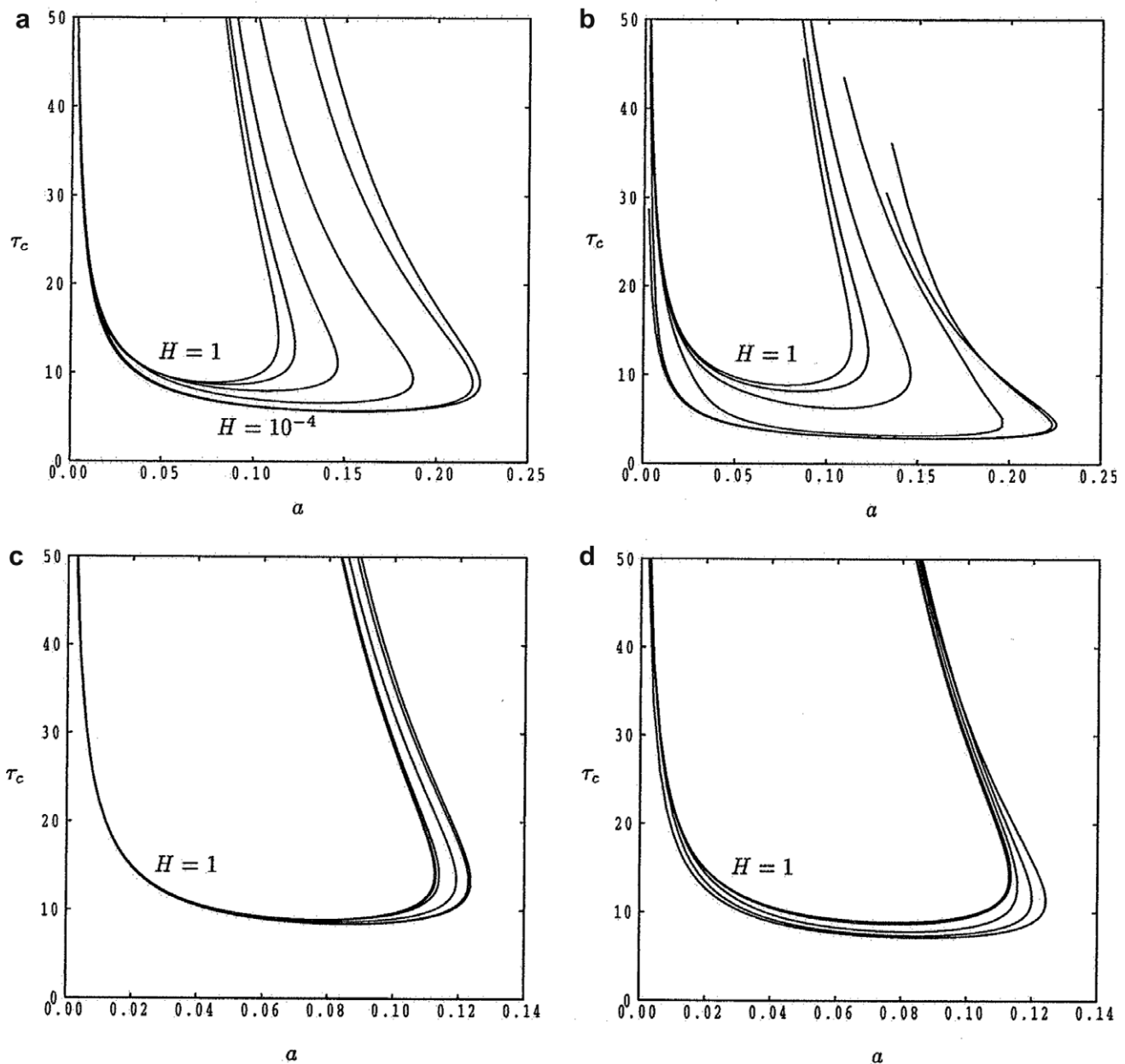


Fig. 3. Neutral stability curves showing the variation of τ_c with the wavenumber, a . Each frame depicts $H = 10^{-n}$ for $n = 0, 1, 1.5, 2, 3$ and 4 : (a) $\alpha = 0.25$, $\gamma = 1$; (b) $\alpha = 4$, $\gamma = 1$; (c) $\alpha = 0.25$, $\gamma = 10$; (d) $\alpha = 4$, $\gamma = 10$.

in terms of both the shape of their profiles and their amplitudes, and the phases tend towards LTE.

For a given value of τ , larger values of H also result in thermal fields that are much closer to one another for the same reason. Although it is perhaps not as obvious, this behaviour also occurs for larger values of γ .

Fig. 2 shows how the situation shown in Fig. 1 changes when α is reduced from 1 to 0.1. Now the diffusivity of the solid phase is much greater than that of fluid phase when $\alpha = 0.1$. The primary difference between Figs. 1 and 2 is the spatial extent of the solid phase disturbance field which now extends well outside, that of the fluid phase. The ratio of the amplitudes of the thermal fields of the phases also remains much larger than when $\alpha = 1$ (see Table 2), although LTE is recovered eventually for the same reasons as given above.

4.2. Neutral curves

Neutral stability curves have been constructed using the detailed evolution of E . Although we are considering a three-parameter problem, a good understanding of how the neutral curves vary with H , γ and α may be gleaned from Fig. 3. These curves display the usual behaviour for a boundary layer, namely one minimum in τ and one maximum in a . At times before the minimum or for wavenumbers greater than the maximum all disturbances are stable (i.e. they decay).

Focussing primarily upon the minimum time for onset for each curve, which we shall call τ_c (and for which the corresponding wavenumber shall be called a_c), it is clear that the decreasing of H towards zero results in the critical time becoming earlier. Whilst this might seem counter-intuitive, it is important to remember that the small- H limit means that the dynamics of the convection are essentially

independent of the solid phase (see Eqs. (17) with $H \sim 0$), and that the equations of motion have been nondimensionalised with respect to the porous medium properties, rather than those solely of the fluid. In their analytical work on the onset of Darcy–Bénard convection with LTNE, Banu and Rees [23] found that the critical Darcy–Rayleigh number reduces towards zero in the same limit, but tends towards a nonzero constant when Darcy–Rayleigh number is based solely upon the fluid properties. Precisely the same applies here in terms of the critical time, and, indeed, it is possible to show that we can reproduce precisely the LTE results of Selim and Rees [16] when the equations are written down in terms of fluid scalings and H is formally set to zero. That this is true is a simple consequence of the fact that the resulting disturbance equations themselves are identical to those of Selim and Rees [16].

At the opposite extreme of large values of H , we recover the results of Selim and Rees [16], but these are in terms of the present scalings, which are based upon the properties of the porous medium. Curves corresponding to larger values of H are almost indistinguishable from the $H = 1$ curves shown.

Figs. 3a and b both represent situations where $\gamma = 1$, but are distinguished by the fact that $\alpha = 0.25$ and $\alpha = 4$, respectively. A large value of α implies that the thermal diffusivity of the fluid phase is greater than that of the solid phase. At early times the basic states for the thermal field of the two phases are given by (14), and it may be seen that, for any chosen time, τ , the thermal boundary layer thickness of the fluid phase increases as α increases. Given that a Rayleigh number based upon the thickness of the fluid thermal boundary layer increases with time and, crudely speaking, has to pass a nominal value before instability occurs, it is clear that the faster development of the

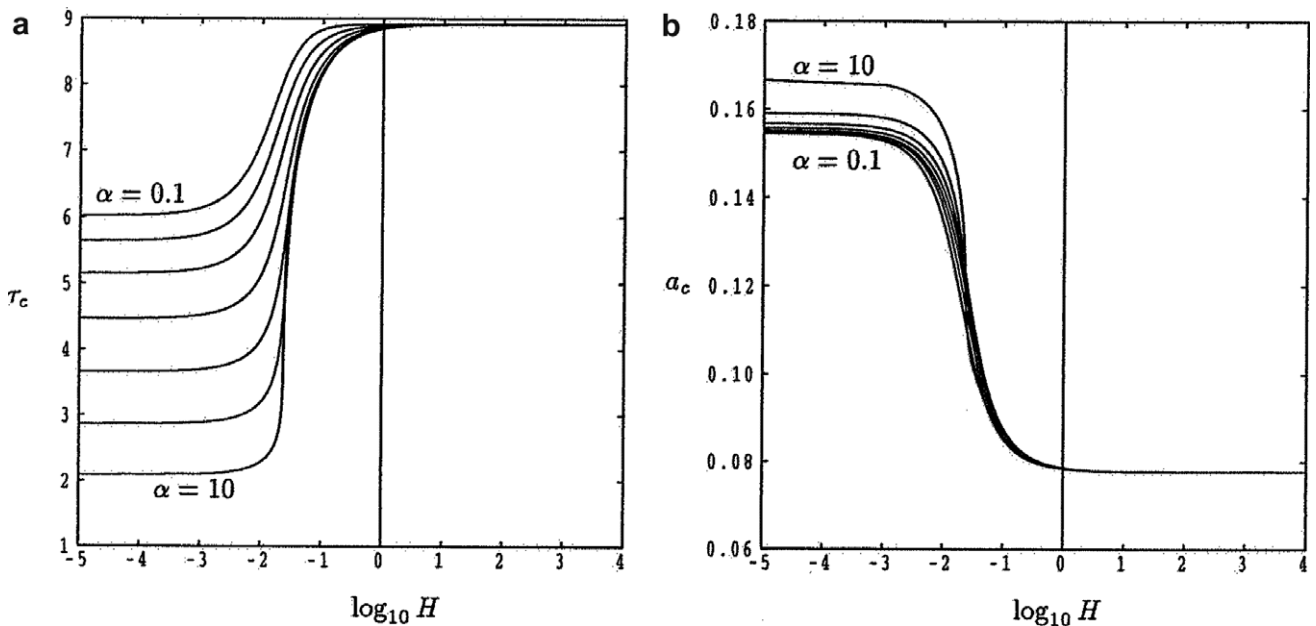


Fig. 4. The variation with H of (a) the critical values of τ and (b) the corresponding wavenumbers for $\gamma = 1$ and for $\alpha = 0.1, 0.25, 0.5, 1.0, 2.0, 4.0$ and 10.0 .

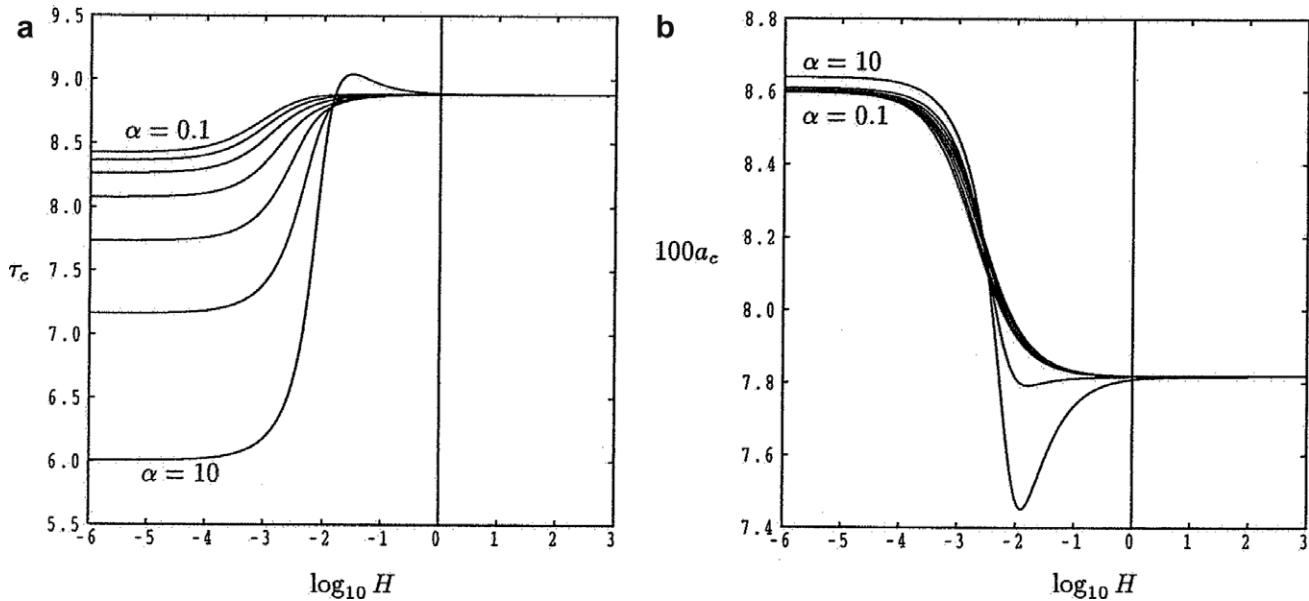


Fig. 5. The variation with H of (a) the critical values of τ and (b) the corresponding wavenumbers for $\gamma = 10$ and for $\alpha = 0.1, 0.25, 0.5, 1.0, 2.0, 4.0$ and 10.0 .

large- α cases must yield small critical times. That this is so is seen readily on comparing corresponding curves between Figs. 3a and b.

The same arguments apply when comparing Figs. 3c and d, which are for $\gamma = 10$. However, the primary difference between this pair of figures and the pair, Fig. 3a and b, is that there is now much less variation between the large- H and the small- H curves. When $\gamma = 10$, the basic thermal boundary layer thickness of the fluid phase varies little when α changes from 0.25 to 4, and this goes some way to explaining why there is only a small variation in the critical time for the onset of convection. A second argument is based upon the fact that the value $\gamma = 10$ increases the dominance of the source/sink term in the solid phase disturbance Eq. (17c). In turn, this means that the solid phase reacts quickly to changes in the fluid phase temperature. Therefore the phases are nearly in LTE, and the neutral curves differ by only a small amount.

Concentrating now on the minimum values of each curve, where $\tau = \tau_c$ and $a = a_c$, Figs. 4 and 5 summarise how these critical values vary with H for a range of values of α , and for $\gamma = 1$ and $\gamma = 10$, respectively. These graphs reveal one feature which was not apparent in Figs. 3a–d, namely the very sharp change in the critical values as H increases from very small values to very large ones. It would appear that this transition is centred very roughly at $H = 10^{-2}$, and that for values of H below this then the phases may be considered to be decoupled, while for values of H above this, then the results of Selim and Rees [16] may be used.

5. Conclusion

In this paper we have extended the analysis of Selim and Rees [16], which gives a detailed account of the onset of

convection in a porous region after the temperature of the horizontal lower bounding surface has been raised suddenly, to cases where the solid and fluid phases of the porous medium are no longer in local thermal equilibrium. To this end we have taken the results of Nouri-Borujerdi et al. [21] as the basic conducting state and have perturbed the full governing equations in a standard linear stability theory. On retaining the time derivatives in the resulting perturbation equations, it has been possible to follow the evolution of disturbances to the basic state and to monitor the response by means of an energy integral. Neutral curves relating onset times with the imposed wavenumber have been presented.

We have found that the presence of LTNE can have a strong influence on the onset of convection. Generally onset occurs earlier when H is small, γ is small or when α is large, as compared with cases when any of these parameters have the opposite magnitudes. The qualitative behaviour for small values of H and γ have been found to be caused by the lack of local thermal equilibrium. However, this behaviour for large values of α is caused by preferential and much more rapid conduction in the fluid phase.

Finally, as with many other works such as Banu and Rees [23], Marafie and Vafai [24] and Minkowycz et al. [25], local thermal equilibrium is always attained when H is sufficiently large. For the present problem, the basic state admits the one-phase complementary error function solution either when H is large or when $\alpha = 1$; in the latter case this is solely because both phases have the same diffusivity and there is no flow. When considering instability, Fig. 4 suggests that LTE is valid when if $H \geq 10$ when $\gamma = 1$ and Fig. 5 yields $H \geq 1$ when $\gamma = 10$. Finally, given the form of source/sink terms in Eqs. (12b) and (12c), which are proportional to $\tau^2 H$, the evolving disturbances enter the LTE regime at a value of τ which is proportional to

$H^{-1/2}$. Therefore LTE is always attained eventually, but this may often be much later than when convective instability arises.

Acknowledgements

The second author (ARN) wishes to express his cordial thanks to the British Council for financial support for his visit to the University of Bath, and to the University of Bath for their hospitality.

References

- [1] H.S. Carslaw, J.C. Jaeger, *Conduction of Heat in Solids*, Oxford University Press, 1986.
- [2] R.H. Socolow, Can we bury global warming? *Scientific American* (July Issue) (2005).
- [3] B.R. Morton, On the equilibrium of a stratified layer of fluid, *J. Appl. Math.* 10 (1957) 433–447.
- [4] T.D. Foster, Stability of homogeneous fluid cooled uniformly from above, *Phys. Fluids* 8 (1965) 1249–1257.
- [5] I.G. Hwang, C.K. Choi, An analysis of the onset of compositional convection in a binary mixture solidified from below, *J. Cryst. Growth* 162 (1996) 182–189.
- [6] C.K. Choi, K.H. Kang, M.C. Kim, I.G. Hwang, Convective instabilities and transport properties in horizontal fluid layers, *Korean J. Chem. Eng.* 15 (1998) 192–198.
- [7] M.C. Kim, K.H. Choi, C.K. Choi, Onset of thermal convection in an initially stably stratified fluid layer, *Int. J. Heat Mass Transfer* 42 (1999) 4253–4258.
- [8] M.C. Kim, T.J. Chung, C.K. Choi, The onset of Taylor-like vortices in the flow induced by an impulsively started rotating cylinder, *Theor. Comput. Fluid Dyn.* 18 (2004) 105–114.
- [9] A.P. Bassom, P.J. Blennerhassett, Impulsively generated convection in a semi-infinite layer above heated flat plate, *Quart. J. Mech. Appl. Math.* 55 (4) (2002) 573–595.
- [10] R.J. Goldstein, R.J. Volino, Onset and development of natural convection above a suddenly heated horizontal surface, *Trans. ASME J. Heat Transfer* 117 (1995) 808–821.
- [11] M. Kaviany, Thermal convective instabilities in a porous medium, *Trans. ASME J. Heat Transfer* 106 (1984) 137–142.
- [12] M.C. Kim, S. Kim, C.K. Choi, Convective instability in fluid-saturated porous layer under uniform volumetric heat sources, *Int. Commun. Heat Mass Transfer* 29 (7) (2002) 919–928.
- [13] M.C. Kim, S. Kim, B.J. Chung, C.K. Choi, Convective instability in a horizontal porous layer saturated with oil and a layer of gas underlying it, *Int. Commun. Heat Mass Transfer* 30 (2) (2003) 225–234.
- [14] M.C. Kim, S. Kim, Onset of convective instability in a fluid-saturated porous layer subjected to time-dependent heating, *Int. J. Heat Mass Transfer* 32 (2005) 416–424.
- [15] A. Riaz, M. Hesse, H.A. Tchelepi, F.M. Orr, Onset of convection in a gravitationally unstable diffusive boundary layer in porous media, *J. Fluid Mech.* 548 (2006) 87–111.
- [16] A.S. Selim, D.A.S. Rees, The stability of a developing thermal front in a porous medium. I. Linear theory, *J. Porous Media*, in press.
- [17] D.A. Nield, A. Bejan, *Convection in Porous Media*, third ed., Springer Verlag, New York, 2006.
- [18] D.A.S. Rees, I. Pop, Local thermal nonequilibrium in porous medium convection, in: *Transport Phenomena in Porous Media III*, Pergamon, 2005, pp. 147–173.
- [19] D.A.S. Rees, Microscopic modelling of the two-temperature model for conduction in periodic and heterogeneous media Invited talk at the meeting ‘Computation of flow and transport in heterogeneous media’ held at the University of Bath, June 19/20 2006, in preparation.
- [20] D.A.S. Rees, Thermal boundary layer instabilities in porous media: a critical review, in: D.B. Ingham, I. Pop (Eds.), *Transport Phenomena in Porous Media III*, Pergamon, 1998, pp. 233–259.
- [21] A. Nouri-Borujerdi, A.R. Noghrehabadi, D.A.S. Rees, The effect of local thermal non-equilibrium on impulsive conduction in porous media 2007, submitted for publication.
- [22] H.B. Keller, T. Cebeci, Accurate numerical methods for boundary layer flows 1. Two dimensional flows, *Proc. Int. Conf. Numerical Methods in Fluid Dynamics*, Lecture Notes in Physics, Springer, New York, 1991.
- [23] N. Banu, D.A.S. Rees, The onset of Darcy–Benard convection using a thermal nonequilibrium model, *Int. J. Heat Mass Transfer* 45 (2002) 2221–2228.
- [24] A. Marafie, K. Vafai, Analysis of non-Darcian effects on temperature differentials in porous media, *Int. J. Heat Mass Transfer* 44 (2001) 4401–4411.
- [25] W.J. Minkowycz, A. Haji-Sheikh, K. Vafai, On departure from local thermal equilibrium in porous media due to a rapidly changing heat source, *Int. J. Heat Mass Transfer* 42 (1999) 2272–2285.